COMPENSATING ELECTRODE ERRORS DUE TO ELECTRODE DETACHMENT IN ELECTRICAL IMPEDANCE TOMOGRAPHY

Yasin Mamatjan[1], Pascal Gaggero[2], Beat Müller [3], Bartłomiej Grychtol[4], and Andy Adler[1]
[1] Systems and Computer Engineering, Carleton University, Ottawa, Canada
[2] Bern University of Applied Sciences, Biel/Bienne, Switzerland
[3] Swisstom AG, Landquart, Switzerland
[4] German Cancer Research Center, Heidelberg, Germany

Abstract: Electrical impedance tomography (EIT) shows a great promise for monitoring pulmonary and cardiovascular functions non-invasively. However, there are some challenges to bring EIT from the laboratory to daily clinical use in intensive care unit (ICU). One of the main challenges is the measurement errors caused by poor contact or detachment of electrodes due to the dynamics of environment and human body. Such errors create large image artifacts and may even lead to misleading results. Thus, there is a need for unsupervised failing electrode identification and electrode error compensation. We developed a novel formulation to compensate for such errors caused by failing electrodes and to eliminate image artifacts in real-time. We tested the error correction algorithms with measurements acquired on a cylindrical tank filled with a conductive saline solution. A test object was placed at different positions inside the tank using a robotic system. For each position, several combinations of disconnected electrodes were tested. The developed algorithm - evaluated by comparing the known test object with the reconstructed images - reduced image artifacts caused by failing electrodes and thus improved the robustness of EIT measurements. The results also demonstrated that the proposed failing electrode compensation strategy was effective up to 6 disconnected electrodes for a 32-electrode EIT system. The proposed strategy can help to use EIT as a practical and robust bedside imaging technique for ventilation monitoring.

1 INTRODUCTION

Electrical impedance tomography (EIT) is a non-invasive method to image conductivity distributions within a body from current injection and voltage measurements made at electrodes attached to the body's surface. EIT shows a great promise for monitoring pulmonary and cardiovascular functions non-invasively. In order to bring EIT from the laboratory to daily clinical use in an intensive care unit (ICU), there remain some challenges to be solved. As a medical equipment, EIT needs to fulfill the requirements of a medical grade instrument including the delivery of clear and robust information. Due to the dynamics of environment and human body in the ICU, one of the main challenges in EIT is poor contact or detachment of electrodes, which will create large image artifacts and may lead to misleading results. Such failing electrodes lead to unusable measurements and cause the failure of EIT image reconstruction, since EIT imaging depends on all electrode data for image reconstruction.

In the literature, several techniques were proposed to detect and compensate failing electrode errors. Adler [1] proposed a method to automatically detect failing electrodes and unreliable measurements by means of finding single electrodes whose readings are inconsistent with the rest. Hartinger *et al* [2] proposed a real-time algorithm to manage failing electrodes based on the reciprocity principle. However, both techniques are most suitable for retrospective analysis. Based on the ideas of Adler [1], we propose a new approach: Prior to the image reconstruction

step, we use the measured data to identify and compensate errors caused by different patterns of failing electrodes. The algorithm was developed and tested using measurements recorded from a cylindrical tank filled with conductive saline solution. Inside the tank, a test object was placed at 121 positions while different scenarios with disconnected electrodes were applied.

2 METHODOLOGY

Our goal was to develop fast and unsupervised methods to identify electrode errors and subsequently compensate them in real-time. The following gives a brief outline of our approach:

(i) acquisition of reference and subsequent measurements from an EIT system, which is described in the Experimental Setup.

(ii) identification of failing electrodes based on knowledge of injection and measurement strategy,

(iii) compensation of measurement errors for all affected electrodes by modeling electrode errors as a priori large measurement noise and incorporating them into image reconstruction process,

(iv) image reconstruction using clean data to obtain better image quality.

2.1 Failing Electrode Detection

The failing electrode detection algorithm is based on the knowledge of the injection and measurement strategy. We used a measurement strategy that records the voltage on all possible pairs of electrodes including the injecting ones, which can be used to estimate the contact impedance. It was experimentally determined that contact impedance values lower than 400 Ω represent well connected electrodes. The impedance threshold value and the knowledge of the injecting pattern allow to identify poorly connected or detached electrodes from the measured data.

2.2 Failing Electrode Rejection

The data $\mathbf{v}$ and image $\mathbf{m}$ are related by a physics model [3], $F(\cdot)$:

$$\mathbf{v} = F(\mathbf{m}) \approx \mathbf{Jm} \tag{1}$$

where $\mathbf{J}$ is the sensitivity (or Jacobian) matrix which linearizes the model at a background (or reference) conductivity $\mathbf{m}_r$, given by:

$$[\mathbf{J}]_{i,j} = \frac{\partial [F(\mathbf{m}_r)]_i}{\partial [\mathbf{m}_r]_j}. \tag{2}$$

By using a common linear differential reconstruction algorithm, images of of conductivity changes, $\Delta\mathbf{m} = \mathbf{m} - \mathbf{m}_r$, can be calculated. In that algorithm, the measured voltages $\mathbf{v}$ needs to be subtracted by a reference data set $\mathbf{v}_r$ ($\mathbf{d} = \mathbf{v} - \mathbf{v}_r$).

$$\Delta\mathbf{m} = \mathbf{Rd}, \tag{3}$$

As reference, each recorded data set can be chosen.

To compensate electrode errors, we interpolate data: $\tilde{\mathbf{d}}$, created by reconstructing a model $\mathbf{m}$,

$$\Delta\mathbf{m} = \mathbf{Rd}, \tag{4}$$

and then projecting the data

$$\tilde{\mathbf{d}} = \mathbf{J}\Delta\mathbf{m} = \mathbf{JRd}, \tag{5}$$

where $\mathbf{R}$ is the reconstruction matrix and $\mathbf{d}$ is the original data with electrode errors. $\mathbf{R}$ needs to be optimized for given errors.

The reconstruction matrix $\mathbf{R}$ can be written as [3]

$$\mathbf{R} = \mathbf{PJ}^T(\mathbf{JPJ}^T + \mathbf{W})^{-1} \tag{6}$$

where $\mathbf{P} = \mathbf{\Sigma}_x$ and $\mathbf{W} = \mathbf{\Sigma}_n$. The matrices $\mathbf{\Sigma}_x$ and $\mathbf{\Sigma}_n$ describe the covariance for the image elements and measurements respectively. Noise variance is assumed to be equal and independent on each channel, so $\mathbf{\Sigma}_n = \mathbf{I}$, which is the identity matrix.

We assume that failing electrodes have high noise, where the errors can be modeled as a prior large measurement noise and incorporated into the diagonal elements of $\mathbf{\Sigma}_n$,

$$\mathbf{\Sigma}_n = \lambda^2(\mathbf{I} + \mu\mathbf{E}_e) \tag{7}$$

where $\mathbf{E}_e$ contains error values that are equal to 1 for bad data points and 0 otherwise. λ is the regularization parameter and μ describes noise to signal ratio.

Thus,

$$\tilde{\mathbf{d}} = \mathbf{JPJ}^T(\mathbf{JPJ}^T + \lambda^2(\mathbf{I} + \mu\mathbf{E}_e))^{-1}\mathbf{d}. \tag{8}$$

We can rewrite the portion of the reconstruction matrix with or without correction respectively as

$$\mathbf{X}^* = (\mathbf{JPJ}^T + \lambda^2(\mathbf{I} + \mu\mathbf{E}_e))^{-1} \tag{9}$$

and

$$\mathbf{X} = (\mathbf{JPJ}^T + \lambda^2\mathbf{I})^{-1}. \tag{10}$$

We propose a fast and efficient way to calculate $\mathbf{X}^*$ given $\mathbf{X}$ by using a general algorithm based on the sequence of rank 1 perturbations [6], we obtained

$$\mathbf{X}^* = \mathbf{X} - \mathbf{X}_i^T \mathbf{X}_i (\mathbf{X}_{ii})^{-1}. \quad (11)$$

where $\mathbf{X}_i$ is a vector for data channel i and $\mathbf{X}_{ii}$ is a diagonal element (of the reconstruction matrix). This is calculated step by step for all measurement points affected by a failing electrode.

2.3 Experimental Setup

For our measurements, we used an EIT system (Swisstom AG, Switzerland) [4] with 32 electrodes and a frame rate of 10-50 frames per second. The electrodes were attached in a plane around a cylindrical tank with a circumference of 90 cm and filled with saline water. As test object, we placed a non-conductive ball (Polyoxymethylene, POM, diameter 45 mm) inside the tank by using a robotic system. The ball was placed on points lying on concentric circles inside the tank with radius 100, 75, 50, 25 and 0 mm. The circles contain 64, 32, 18, 8 or 1 equally spaced measurement positions respectively. This leads to a total 121 different object positions. Additionally, reference measurements ($\mathbf{v}_r$) with no ball inside the tank were taken. For the analysis in this paper, we restricted the measurement positions to 8 equally-spaced points lying on the circle with radius 75 mm. For each position, several failing-electrode patterns were applied before measuring, which included 1, 2, 3 and 6 disconnected electrodes.

2.4 Data Processing

We carried out tests and data analysis in MATLAB (Mathworks, Natick, MA) and EIDORS 3.6 [5]. We used the GREIT image reconstruction algorithm [5] with standard settings ($NF = 0.5$, [3]). The forward model used for GREIT is a 3D-FE model of the tank, as described in the previous section. For the case of no failing electrodes, a reconstruction matrix was pre-calculated using the GREIT algorithm. For each case of failing electrodes, we used eq. (7) – (10) to adapt this matrix.

The used EIT system showed an amplifier saturation such that if an electrode failed, the next neighboring electrode was also affected due to current injection from neighboring electrodes. This system specific issue increased the number of total affected electrodes. All measurements except the affected measurements from the failing electrode and its next neighbor electrode with injecting current were considered. This used more of the measurement data. We called the neighboring case *full comp*, while the compensation of the failing electrodes only was called *part-comp*.

3 RESULTS

Sample reconstructed images from the failing electrode study are presented in Fig. 1. These images are based on the measurement data of only 8 object positions with 1, 2, 3 or 6 failing (disconnected) electrodes. To reconstruct the images, the algorithm was extended with different compensation strategies. For all failing electrode cases, the reconstruction failed to produce proper images when no compensation was performed (*no-comp*). Since the failing electrodes were detached and kept open, they have random noise values, and thus the reconstructed images varied in different cases and image artifacts were not proportional to failing electrodes. Image artifacts are reduced considerably after applying compensation for the failing electrodes (*part-comp*) only. Finally, we successfully compensated the failing electrode as well as the affected neighboring (current injection) electrodes (*full-comp*), where the image quality dropped gradually for the increased number of failing electrodes due to the reduced number of measurements.

4 DISCUSSION

We proposed strategies for compensating electrode errors to reduce image artifacts. In all our analysis, the electrode error compensation strategies kept the EIT system functioning properly in the presence of up to 6 failing electrodes and improved the image quality considerably. The approach also allows fast processing. In this study, the failing of 6 electrodes resulted in a loss of 8 measurement/injecting pairs due to the distribution pattern of the failing electrodes. If distributed in another pattern, this may end in a loss of up to 12 pairs. Further clinical studies are needed (with human subjects) to improve the proposed compensating strategy for multiple failing electrodes, i.e. by using adaptive injection patterns.

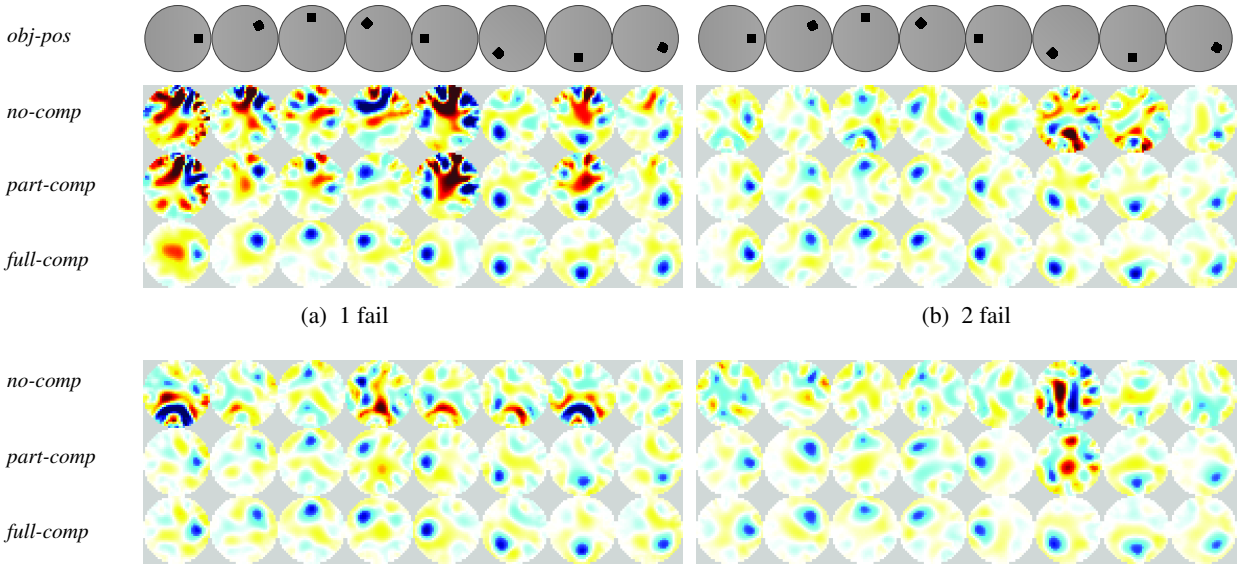

Figure 1: Reconstructed images based on different compensating strategies for failing electrodes: (a) 1 failing electrode, (b) 2 failing electrodes, (c) 3 failing electrodes, (d) 6 failing electrodes. *obj-pos* stands for real object position, *no-comp* is for no compensation, *part-comp* is for electrode error compensation, *full-comp* is for compensating electrode errors and additionally the errors from next (current injection) electrode.

For the practical application of EIT, patient movement and poorly contacting electrodes are unavoidable. The image artifacts or failure of the image reconstruction caused by them may lead to misleading visual results and subsequent faulty diagnosis. The proposed approach can identify and compensate electrode errors in real-time. Thus, the method improves the stability of EIT measurements, and increases the efficiency and reliability of an EIT system especially for long term bedside monitoring of patients.

ACKNOWLEDGEMENTS

This work was funded partly by the Swisstom AG (Landquart, Switzerland). P. Gaggero was supported by the Swiss Commission for Technology and Innovation (CTI Medtech Project No. 12888.1 VOUCH-LS). B. Grychtol was supported by a research fellowship from the Alexander von Humboldt Foundation.

References

[1] A. Adler, "Accounting for erroneous electrode data in electrical impedance tomography," *Physiol. Meas.*, vol. 25, no. 1, pp. 227-238, 2004.

[2] A. E. Hartinger *et al*, "Real-time management of faulty electrodes in electrical impedance tomography," *IEEE Trans. Biomed. Eng.*, vol. 56, no. 2, pp. 369-377, 2009.

[3] A. Adler and R. Guardo, "Electrical impedance tomography: regularised imaging and contrast detection," *IEEE Trans. Med. Imaging*, vol. 15, pp. 170–179, 1996.

[4] P. Gaggero *et al*, "Electrical impedance tomography system based on active electrodes," *Physiol. Meas.*, 33:831847, 2012.

[5] A. Adler and W.R. Lionheart, "Uses and abuses of EIDORS: An extensible software base for EIT," *Physiol. Meas.* 27:S25-S42, 2006.

[6] C. Gómez-Laberge and A. Adler, "Direct EIT jacobian calculations for conductivity change and electrode movement," *Physiol. Meas.*, vol. 29, pp. 89–99, 2008.